**Article:**

Nanayakkara, K.I.U. orcid.org/0000-0003-2630-7724, Liew, A. and Gilbert, M. (2025) Thrust layouts in masonry gravity structures. International Journal of Solids and Structures, 323. 113593. ISSN: 0020-7683

https://doi.org/10.1016/j.ijsolstr.2025.113593

# Thrust layouts in masonry gravity structures

K. Isuru U. Nanayakkara[a,], Andrew Liew[b], Matthew Gilbert[a]

[a] *School of Mechanical, Aerospace and Civil Engineering, The University of Sheffield, Mappin St, Sheffield, S1 4DT, South Yorkshire, United Kingdom*
[b] *Unipart Construction Technologies, Advanced Manufacturing Park, Catcliffe, Rotherham, S60 5WG, South Yorkshire, United Kingdom*

**Abstract**

Heyman's 'safe theorem' is widely used to assess the safety of masonry gravity structures. In its original incarnation, a funicular thrust line—i.e., a hanging chain—was used to represent a possible flow of forces through a structure, though this was later found to be problematic in some cases. Following the work of Moseley, a line of resistance has also been used as a representation of a thrust line. However, although this provides a valid representation of equilibrium, it does not facilitate clear visualization of a flow of forces within a structure, making it less intuitive than a funicular thrust line. To address shortcomings associated with funicular thrust lines, the notion of a 'thrust layout' is also considered here. This can accurately represent a state of equilibrium while also enabling visualization of the flow of forces. Thrust layouts also allow explicit consideration of the tensile forces that can (or cannot) be reasonably sustained in a masonry construction, such as within constituent blocks but not across weak joints.

*Keywords:* Form-resistant structures, thrust lines, thrust layouts

## 1. Introduction

Robert Hooke (1635-1703) observed the correspondence between a hanging chain and a rigid arch and stated 'As hangs the flexible line, so but inverted will stand the rigid arch' [1, 2, 3]. Thus originated the idea of a 'funicular' to represent the equilibrium of an arch. In 1748, Poleni successfully applied this to the analysis of the cracked dome of St. Peter's in Rome [3].

*Email address:* `isuru_nanayakkara@live.com` (K. Isuru U. Nanayakkara )

Since then, thrust lines generated from funiculars have been extensively used in the analysis of masonry gravity structures, such as arches, vaults, and domes. Here, such thrust lines generated from funiculars will be referred to as 'funicular thrust lines', where the funiculars can be from physical hanging chain/cloth models [4, 5, 6], graphic statics [2, 5, 7, 8], or various other numerical methods (e.g., particle spring models [9, 10]). The usage of funicular thrust lines was further popularized by the development of Heyman's 'safe theorem' [1], as this placed it within the realm of limit analysis, giving structural engineers the confidence to use it in everyday practice. Here, it is noted that a thrust line may not represent the exact state of the structure, where these masonry gravity structures are highly statically indeterminate a thrust line would only show one possible flow of forces within the structure. As Heyman [11] notes, and experimental evidence suggest [12], this is sufficient to guarantee the safety of masonry gravity structures.

However, as was later noted by Heyman himself [13, 14], along with others, funicular thrust lines unintentionally assume the structure to be made up of equivalent vertical strips of material, rather than using the actual block stereotomy that is present. If care is not exercised then this assumption may lead to unsafe designs. For instance, when analysing a masonry buttress, the masonry effective in resisting the external loads needs to be determined first to prevent ineffective material from being inadvertently 'lifted up' to the thrust line, leading to an overestimation of the load carrying capacity [12, 15].

The usage of thrust lines is further complicated by the different notions of thrust lines that arise from Moseley's 'line of resistance' and 'line of pressure', where the latter coincides with what is here referred to as a funicular thrust line [3, 16]. Although the subtle but important distinctions between the two have been previously noted, they have both been referred to as 'thrust lines'[1], and used in the application of Heyman's safe theorem (e.g., the line of resistance is used as the thrust line in [5, 17, 18], whilst the line of pressure / funicular thrust line is used for this purpose in [2, 11, 19])

Drawing upon previous attempts to resolve these issues ([13, 16, 20]), a thorough discussion is provided here. In addition, the new notion of a 'thrust

[1] In this paper, the term 'thrust lines' is used as an umbrella term for all usages of thrust lines. Furthermore, 'thrust lines' and 'lines of thrust' are considered interchangeable terms, referring to the same.

layout' is introduced, which allows new light to be shed on the various definitions of thrust lines. Thrust layouts are a valid representation of equilibrium (as is the line of resistance) and a valid force flow (as is the line of pressure/funicular thrust line) of masonry gravity structures, thus providing a means of bringing together the current competing definitions.

Issues related to frictional contacts in thrust lines are noted but not explored in depth in this work. Heyman's safe theorem assumes infinite friction capacity at masonry block interfaces, notwithstanding that frictional failures in masonry gravity structures have been previously observed, e.g., sliding failure at the head of a flying buttress [21]. In this case, Bagi [22] has pointed out that rigid block systems can fail even when an equilibrium solution exists and the sliding resistance is not exceeded anywhere, with additional kinematic conditions needing to be considered to make Heyman's safe theorem truly 'safe' in this case. Furthermore, other failure modes such as creep instability and crushing at hinge points are also ignored [23].

In this contribution, the limitations of using funicular thrust lines are first carefully considered. Then, to remedy these, thrust layouts are introduced. Conjectures on detecting valid and erroneous funicular thrust lines are also presented. An example of a flat arch on two columns is presented to demonstrate the superiority of the proposed thrust layouts in comparison to the funicular thrust lines.

## 2. The funicular thrust line

A funicular thrust line (or a 'line of pressure') is defined here as a funicular polygon representing a possible state of equilibrium of a masonry gravity structure. These terms are formally defined as follows.

**Definition 1.** *A* ***funicular polygon*** *is an open or closed polygon that takes the form of a (weightless) cable acted upon at a number of points by forces in various directions. (see Fig. 1)*

**Definition 2.** *A* ***funicular thrust line*** *is a funicular polygon, where the forces acting upon the cable represent the boundary conditions of a masonry gravity structure (i.e., external loading, self-weight, and support reactions), and the cable represents one possible state of equilibrium of the masonry gravity structure.*

Figure 1: A funicular polygon generated by hanging loads on a cable or thread (in blue), the weight of which is negligible.

Jacques Heyman, in his eponymous 'safe theorem', used funicular thrust lines to represent the equilibrium of a masonry gravity structure [1], with the zero tensile capacity yield criterion satisfied when these thrust lines are completely contained within the extents of the structure. Thus, if a funicular thrust line subjected to self-weight and external loading can be contained entirely within the structure, it can be deemed safe; see Fig. 2.

### *2.1. Assumption of equivalent vertical-strips*

Heyman [13] notes that his earlier work [1] "unintentionally" assumes the voussoirs to have vertical cuts between them. He concludes that, although the safe theorem can reasonably be applied to say, a monolithic arch, it fails to account for the effects of cuts, or interfaces between voussoirs (*la coupe des pierres* or block stereotomy).

For instance, consider the segmental arch shown in Fig. 3. A funicular thrust line, shown in blue is generated considering the weight of the voussoirs, lumped at their mass centres. The geometry of the real voussoirs, and the

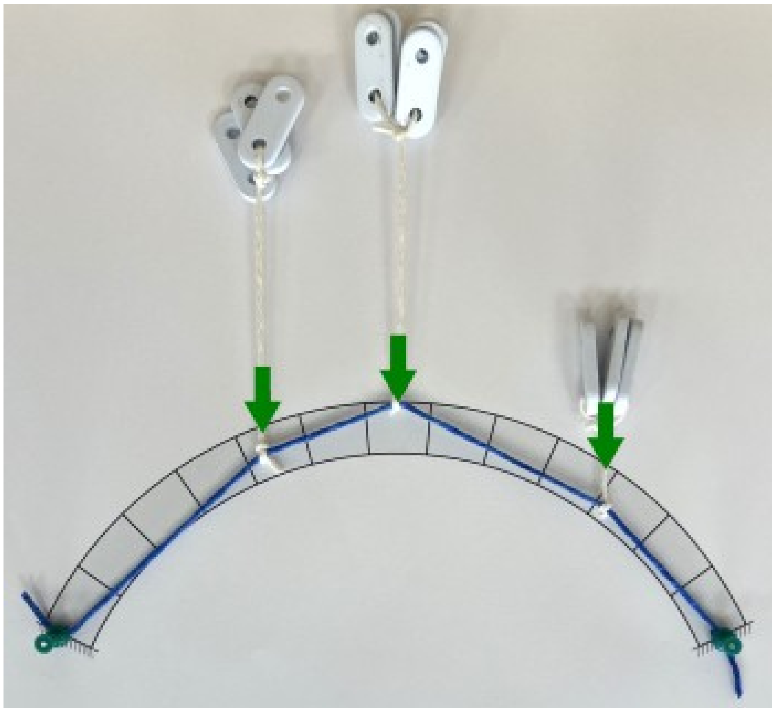

Figure 2: Heyman's safe theorem: the funicular thrust line (in blue), generated by a hanging chain model (inverted), is fully contained within the arch section; assuming the self-weight of the arch is negligible, the arch can be considered safe.

corresponding equivalent vertical strips (in grey) for two voussoirs, A and B, are shown.

Now consider the funicular thrust line segments within those voussoirs, real and equivalent, and the corresponding thrusts at their interfaces (see the inset figures in Fig. 3b). As seen in inset (i), the thrust line segment within the voussoir (blue line) and the thrusts at the interfaces (green arrows) do not exactly coincide, leaving an offset; i.e., they are inconsistent, albeit only slightly. This inconsistency implies that the funicular thrust line is not a valid representation of the equilibrium of the voussoir, and thus the arch. In contrast, the funicular thrust line and the thrusts at interfaces are consistent for the equivalent vertical strips (see inset (ii) of Fig. 3b).

Nevertheless, the geometry and orientation of the voussoirs can be such that the static equilibrium representation of a thrust line is still valid. For instance, consider voussoir B in Fig. 3. As seen in inset (iii) the funicular

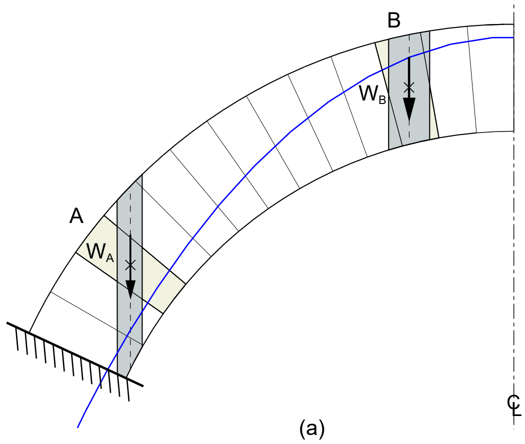


(a)

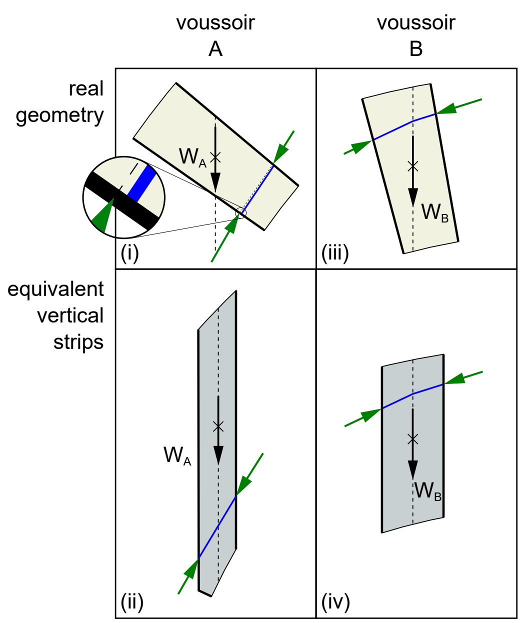


(b)

Figure 3: Funicular thrust lines unintentionally assume a series of equivalent vertical strips instead of the actual voussoir stereotomy: funicular thrust line within voussoir A is not consistent with the thrust at the interfaces, whereas it is for the assumed equivalent vertical strip; in contrast, for voussoir B, the funicular thrust line within both the voussoir and the equivalent vertical strip are consistent with the thrust at interfaces.

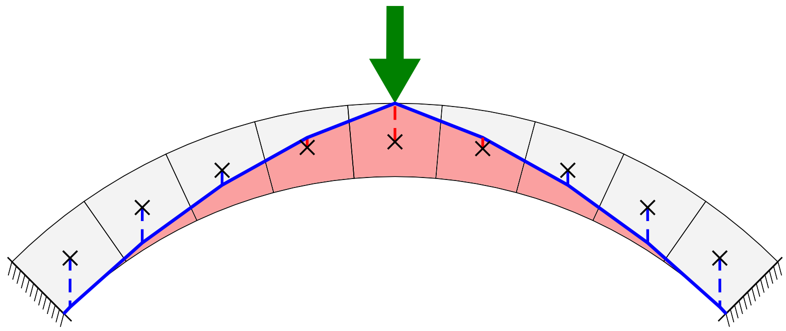

Figure 4: Implicit tension in funicular thrust lines: Funicular thrust lines assume tensile forces to transfer the self-weight loads from their points of application to the thrust line, as indicated by dashed red verticals where the self-weights are lumped at the centres of mass of the voussoirs. Equivalently, when the self-weight is considered distributed, the areas below the funicular thrust line (shaded in pink) will be in tension in the vertical direction. Similarly, blue indicates compressive forces.

thrust line and the thrusts at interfaces are in this case consistent. This is in fact guaranteed to be the case if the line of action of the self-weight of the voussoir does not cross a radial joint (i.e., the line of action of the self-weight remains within the corresponding block).

### *2.2. Implicit tensile strength*

Now consider the segmental arch shown in Fig. 4. A funicular thrust line, corresponding to one possible flow of forces, is also constructed, shown in a blue solid line, considering self-weights lumped at the centres of mass of the voussoirs.

Now observe in Fig. 4 the positions of the centres of mass (marked with an $\times$) relative to the funicular thrust line. It is evident that some of the mass centres lie above the funicular thrust line, while others lie below. This implies that struts in compression are required to transfer the self-weight of voussoirs to the thrust line, as indicated by dashed blue vertical lines running from the centres of mass in Fig. 4. Similarly, ties in tension are required to transfer the self-weight loads in cases where the centres of mass of voussoirs are below the funicular thrust line; see dashed red vertical lines in Fig. 4. Thus, this construction of a funicular thrust line implicitly assumes that tensile forces can be resisted by the masonry.

In summary, funicular thrust lines (i) assume equivalent vertical strips instead of the real voussoir configuration, which is likely to lead to an invalid representation of the state of equilibrium of the structure; and (ii) implicitly assume tensile forces can be resisted by the voussoirs, although this is not made explicitly clear to the users, though no tensile forces are allowed in the funicular thrust line itself.

For a typical example involving a segmental arch subjected to self-weight and other vertical loads, the aforementioned shortcomings may lead to conservative predictions of safety. Consider for example the two voussoirs shown in Fig. 5, where the voussoirs share a common interface, have self-weights $W_A$ and $W_B$, and are subjected to thrust forces $\mathrm{F}_A$ and $\mathrm{F}_B$. Here, the funicular thrust line considered (and shown in a solid blue line) moves outside the two-voussoir configuration indicating according to Heyman's safe theorem that the structure will not stand due to the absence of a valid equilibrium solution. However, the structure is safe: the three forces on each of the voussoirs (self-weight, external thrust force, and the thrust between the voussoirs) create closed force polygons (see force diagram in Fig. 5) guaranteeing equilibrium, and all thrust forces are contained within corresponding interfaces ensuring the yield condition for masonry is not violated. Thus, here, the funicular thrust line indicates an unsafe structure even when the structure is safe, therefore leading to a conservative assessment of safety.

Alternatively, assuming infinitely rigid blocks (which was not an explicit assumption of Heyman [1]) would rectify the issues caused by the assumption of vertical strips and implicit tensile strength [24]. However, thrust lines generated with this assumption would no longer be funicular thrust lines: they would align with the notion of the line of resistance, described next in Section 3.

## 3. The line of resistance

In 1843 Moseley [25] presented the notion of a 'line of resistance' to represent a possible state of equilibrium of 'a structure made of uncemented stone'. The same notion was in 1907 also presented by Milankovich, though in this case referred to as *die druckkrve* [26, 27]. When thrust lines are presented from rigid block analysis (e.g. [18]), this notion of a line of resistance is being used.

**Definition 3.** *A **line of resistance** is a geometrical locus of points-of-application of the resultant thrust forces that develop at interfaces within a masonry arch or other structure.*

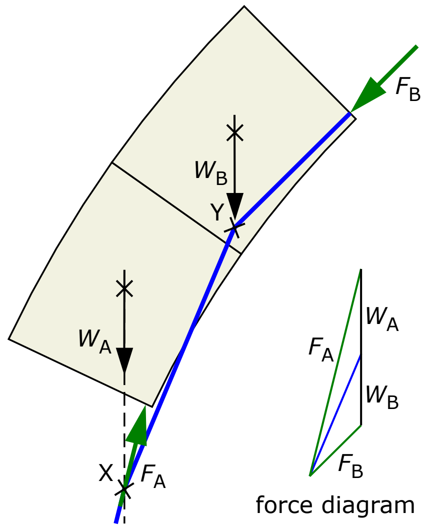


Figure 5: Funicular thrust line in two-voussoir example: although an equilibrium solution exists, the funicular thrust line moving outside the extent of the assembly indicates an unsafe solution. (The two voussoirs are of weight $W_A$ and $W_B$, share an interface, and are subjected to thrusts $F_A$ and $F_B$.)

Revisiting the two-voussoir example, now consider a line of resistance. The line of resistance drawn as a solid purple line in Fig. 6 is constructed by first determining the points-of-application of thrust at each interface (marked X, Y, Z) and then connecting them by line segments.

Thus a line of resistance is a valid equilibrium representation that explicitly considers block stereotomy. However, it does not necessarily align with the thrust trajectory at interfaces; this happens if and only if the interfaces are vertical [26, 27]. Thus, it can be argued that a line of resistance does not represent a valid force flow within the structure. Also, as a line of resistance does not follow the thrust force vectors, it is visually less intuitive than a funicular thrust line and does not make it clear to a structural engineer how the structure could safely carry the applied loads.

Furthermore, a convenient, albeit non-rigorous, way of checking for sliding failure is to check the angle of incidence of a thrust line at an interface against the angle of friction of the material; e.g., see [25, 28]. Now, since a line of resistance representing a thrust line does not reflect the actual thrust trajectory, such a geometrical check is not possible.

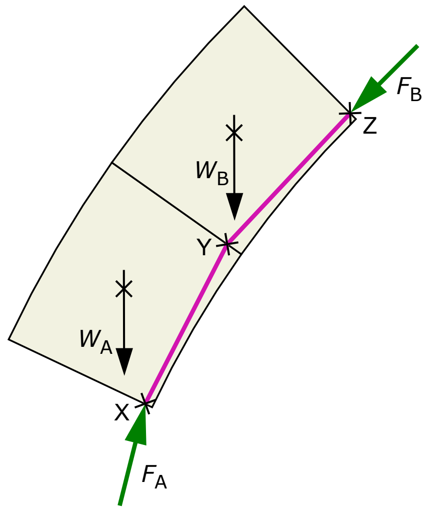


Figure 6: Line of resistance in two-voussoir example: although the line of resistance is fully contained within the structure, it does not correspond to a force flow as the line segments do not align with the corresponding thrusts at the interface.

## 4. The thrust layout

Now, consider the network of forces in Fig. 7 for the same two-voussior example considered earlier. The network is fully contained within the structure; its line segments align with the force vectors and the forces satisfy equilibrium constraints for each of the voussoirs, and hence in turn the whole assembly. Therefore, this network of forces is both a valid representation of equilibrium and a meaningful visualisation of force flow. This network of forces is here termed the 'thrust layout'.

The thrust layout is formally defined below:

**Definition 4.** *A* ***thrust layout*** *is a network of forces in equilibrium, representing a possible flow of forces in an assembly of blocks, where:*

1. *compressive forces of any magnitude are allowed;*
2. *self-weight forces must be transferred to the network within the extent of the corresponding masonry block;*
3. *tensile forces are allowed within blocks, but not across the weak interfaces that lie between them.*

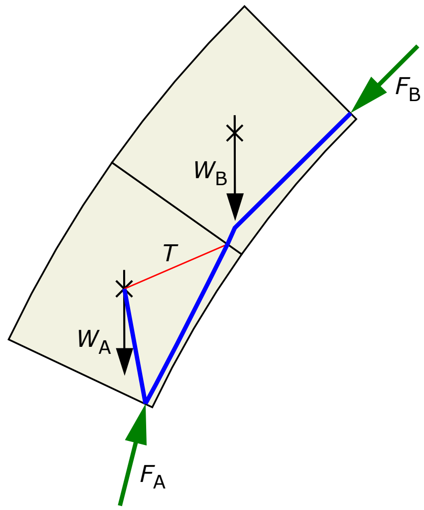


Figure 7: Thrust layout in two-voussoir example: the thrust layout is fully contained within the structure and properly corresponds to a force flow (Blue and red lines correspond to compression and tensile forces, respectively).

Taking a thrust layout to be a natural extension of a funicular thrust line, the condition of infinite compressive forces is adopted here and two additional constraints are introduced: (i) self-weight is assumed to be transferred to a thrust layout within the extent of a given block; (ii) tension is explicitly allowed within the extents of a given block. The effects of these additional constraints are explored further in the following sections.

### *4.1. Transferring self-weight to the thrust layout within the extent of a given block*

Consider the simple two-block example shown in Fig. 8a, which shows a small block stacked on a larger block. An increasing horizontal load $P$ is applied at the top left corner of the top block, which will eventually overturn that block about its bottom right corner, opening up the weak interface between the two blocks. One may construct a hanging chain model (Fig. 8b), or a corresponding graphic static funicular thrust line (Fig. 8c), considering the self-weights of the blocks, $W_A$ and $W_B$, to be lumped at their mass centres. Both methods predict the same collapse load, of $P = P_1$.

However, the force flow represented by this funicular thrust line is not admissible in the real structure, since it implicitly assumes that a tensile

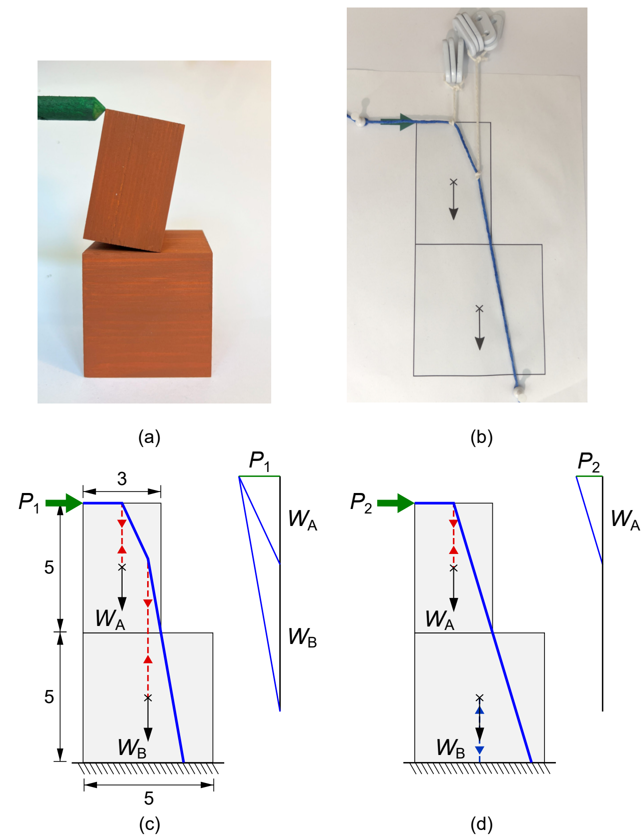


Figure 8: Mobilizing self-weight load within the extent of a given block: (a) experimentally observed failure mechanism when a horizontal load $P$ is applied at the top left corner of the top block; (b) physical hanging chain model at failure, with $P = P_1$; (c) corresponding graphic statics model, with again $P = P_1$; (d) thrust layout model, with now $P = P_2$, where $P_2 < P_1$; in this case the self-weight of the bottom block is carried directly by the supporting ground whereas the funicular thrust line implicitly assumes that a tensile force can be transmitted across the weak interface between the blocks, inadmissible in the physical model. (Compression and tension forces are shown in blue and red respectively. For $W_A$ and $W_B$ of 15 and 25 units, $P_1$ and $P_2$ are 7 and 4.5 units, respectively.)

force can be transmitted across a weak interface, which in reality is not possible. This error is easily detected when the forces carrying self-weight from the mass centres to the funicular thrust line are plotted (see Fig. 8c), whereas not so obvious in the physical hanging chain model (see Fig. 8b).

This erroneous funicular thrust line can be corrected by ensuring the self-weight load corresponding to a given block is mobilized only within the extent of that block. A valid thrust layout is presented in Fig. 8d, where the self-weight of the bottom block $W_B$ is not transmitted up to the main thrust line, but instead is directly transferred down to the supporting ground. In this solution equilibrium of each individual block is satisfied, and hence so is the equilibrium of the whole structure. Also, the yield condition is satisfied at all interfaces (i.e., no tension is applied across weak interfaces), with the solution also corresponding to a valid collapse mechanism, where the top block rotates about the bottom right corner, as in Fig. 8a, thus giving the exact collapse load, of $P = P_2$.

Contrary to the commonly held belief that thrust line solutions will always be conservative, the solution of $P = P_1$ given by the funicular thrust line in Fig. 8c, is higher than the exact collapse load of $P = P_2$, since the self-weight of the bottom block will help resist the applied load.

### *4.2. Incorporating tension explicitly*

Now consider another example involving two blocks, where in this case the top block overhangs the bottom block (Fig. 9a). The two block assemblage is in this case subjected to an inclined load applied to the top right corner of the overhanging block.

Firstly, an attempt is made to construct a funicular thrust line for this example (Fig. 9b). For this, a compressive force along the line of action of the external load $P$ is required, to satisfy equilibrium at point X. However, this compressive force would move outside of the structure before intersecting the line of action of the self-weight $W_A$ of the top block (indicated by a dashed line). Thus a funicular thrust line fully contained within the structure cannot be constructed.

Yet the physical model (Fig. 9a) suggests that a valid solution must exist. Investigating this further, a free body diagram for the rocking top block is drawn (Fig. 9c); observe the top block rocking about point Y in the physical model. This is equivalent to a beam subjected to a point load in bending. The presence of bending in the beam suggests that tensile forces must be mobilized in the block, likely to be in the upper portion of the block. Following this intuition, a force network that includes a tensile force (i.e., a thrust layout) is constructed (Fig. 9d), where the forces are in equilibrium and the network is fully contained within the structure.

Thus, a valid thrust layout is constructed by explicitly allowing tensile forces within constituent blocks to mobilize self-weight within the extent of the corresponding blocks. A valid thrust layout exists although a funicular

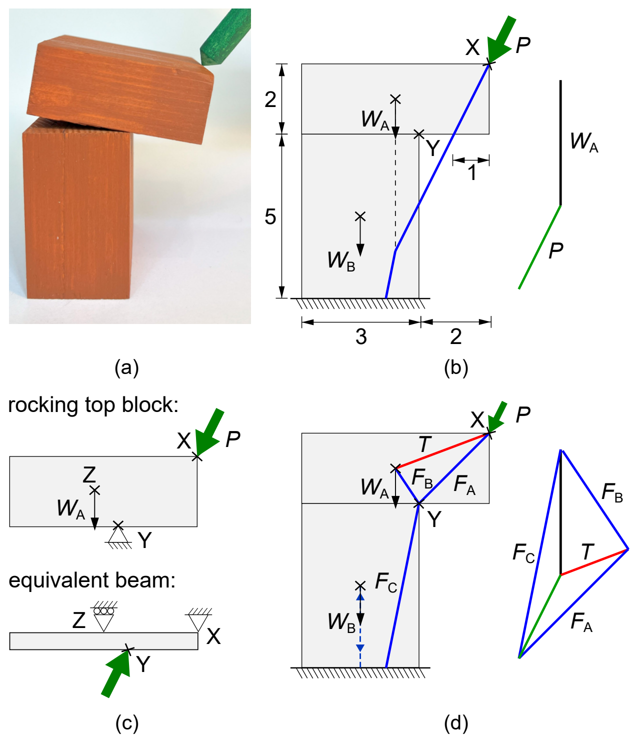


Figure 9: Incorporating tension explicitly: (a) experimentally observed failure mechanism when an inclined load $P$ is applied at the top right corner of the top block; (b) a thrust line lying entirely within the structure cannot be constructed; (c) observing the equivalence of the rocking top block (in the physical model) to a beam in bending, the requirement for tensile forces to be present inside the block is noted; (d) a valid thrust layout incorporating tensile forces is constructed. (Compression and tension forces are shown in blue and red respectively. For $W_A$ and $W_B$ of 15 and 10 units, $P$ and $T$ is 5.6 and 2.5 units, respectively.)

thrust line has suggested an unstable structure under the given loading. Note that the thrust layout presented in Fig. 9d is one of many possible valid thrust layouts.

## 5. Identifying erroneous funicular thrust lines

Funicular thrust lines have traditionally been used to analyze masonry gravity structures, and structures built based on such analysis still exist. It will be useful to formally check if those funicular thrust lines give safe results and correct them when not. The following discussion forms a basis towards that end.

### *5.1. When the funicular thrust line is valid*

Funicular thrust lines give an invalid representation of equilibrium when, at an interface, the point of action of the thrust and the point of intersection of the funicular thrust line with the interface are not coincident. As observed previously, this occurs when the self-weight loads are transferred to the thrust line at a point outside the corresponding block (see Fig. 3). This is now studied in detail, additionally considering the following simplifying assumptions.

- Only three forces, self-weight and externally applied loads and/or thrusts at interfaces, are applied on each of the constituent blocks, therefore requiring the lines of action of those forces to coincide at a point to ensure equilibrium of the block.
- The block is convex, or only slightly concave, therefore having the self-weight's line of action intersecting the block's boundary only at two points: at an upper and lower interface.
- Block interfaces are perfectly flat.

These assumptions are reasonable and valid for the typical structures and loading cases studied with funicular thrust lines.

Consider a constituent block of a block assembly in isolation: see Fig. 10. The point of intersection of the lines of action of the three forces (herein referred to as point X) can be within, above, or below the block. Here, 'above' and 'below' are with respect to the segment of self-weight's line of action which is within the block's boundary and the gravity direction being vertically downward (see Fig. 11).

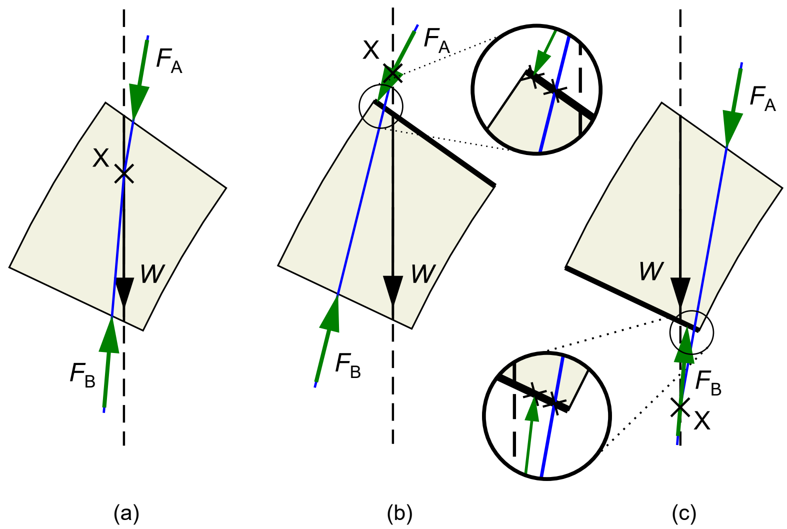


Figure 10: Equilibrium of a block subjected to three forces ($F_A$, $F_B$, and $W$): The point of intersection of their lines of action (point X) can be (a) within, (b) above, or (c) below the block.

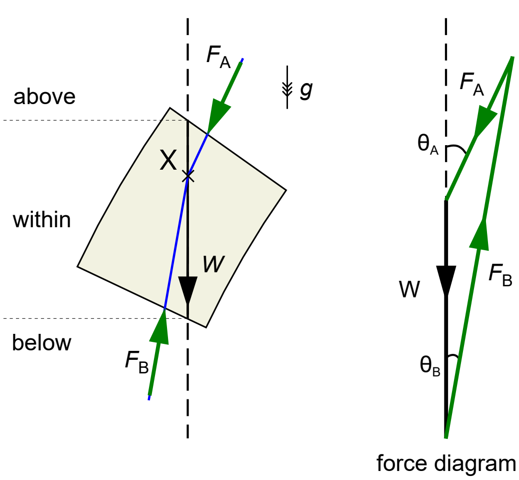


Figure 11: Form and force diagram of a block subjected to three forces ($F_A$, $F_B$, and $W$). Given the gravity direction is vertically downward, the force 'above' ($F_A$) will make a larger angle with the vertical than the force 'below' ($F_B$); $\theta_A > \theta_B$.

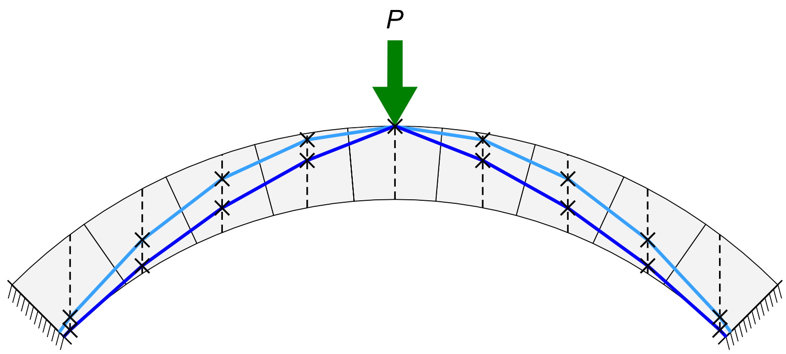


Figure 12: When the funicular thrust line is valid: If the segment of the self-weight's line of action which is within the extent of the structure (dashed vertical lines) is also fully within the corresponding block, then any funicular thrust line for the structure (solid lines in blue) which are contained within the structure will be a valid representation of equilibrium. The funicular thrust line is light blue for $P = 0$ and the darker blue is for $P_{limit}$. Points X are marked with crosses.

Looking at Fig. 10a, any combination of thrusts ($F_A$ and $F_B$) with point X inside the block will give a thrust line segment (in blue) consistent with the thrusts at interfaces. Thus we conjecture the following:

**Conjecture 1.** *Given only three forces are applied on each of the blocks of a block assembly, if the segment of the self-weight's line of action which is within the extent of the structure is also fully within the corresponding block, then any funicular thrust line for the structure which is contained within the structure will be a valid representation of equilibrium for the structure.*

Points X will always be (a) on the line of action of the self-weight of the corresponding block, and (b) on the funicular thrust line ($\because$ a polygon on the force diagram is a point on the dual form diagram). Then, (a) the segment of the self-weight's line of action which is within the extent of the structure being also fully within the corresponding block, and (b) the funicular thrust line considered being fully contained within the structure results in the point X being within the corresponding block. This, then guarantees that the block under consideration is some version of the case shown in Fig. 10a. This ensures that the thrusts at the block interfaces are consistent with the funicular thrust line. Fig. 12 is an example of the above being the case for all blocks, and therefore satisfying the conditions of Conjecture 1.

Note that the Conjecture 1 gives a sufficient condition for a funicular

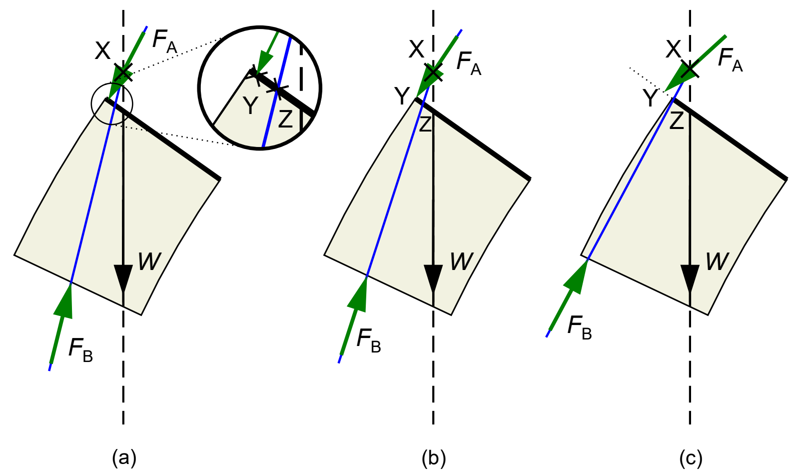


Figure 13: When point X is above the block: The lines of action of the equilibrating forces $F_A$, $F_B$, and $W$ on the block intersect at point X. The point of action of the thrust $F_A$ is point Y and the funicular thrust line intersects the interface at point Z. In (a) both points Y and Z are inside the structure; (b) point Y is at the boundary of the structure; (c) point Y is outside the structure while point Z is still inside the structure. In all cases the funicular thrust line is inside the structure

thrust line to represent equilibrium accurately. However, it is not a necessary condition.

### *5.2. Collapse load over-estimation*

Now, consider the scenario from Fig. 10b when point X is above the constituent block. Point X must be inside the structure, otherwise the funicular thrust line is already indicating an unsafe structure.

The free-body diagram and the funicular thrust line in Fig. 10b are reproduced in Fig. 13a, now with two more cases. It presents possible cases for the point of action of the thrust $F_A$ when point X is above the block and the funicular thrust line inside the structure. Here, without loss of generality, the three cases are generated by increasing the horizontal component of the thrust $F_A$ while point X is kept in place.

In Fig. 13, the point of action of the thrust $F_A$ at the upper interface (in bold) is denoted point Y (see inset), and the point of intersection of the funicular thrust line with the interface is denoted point Z. Following from the force diagram in Fig. 11, thrust $F_A$ makes a larger angle to the vertical compared to that of thrust $F_B$. Observe that when point X is above the block, the segment of the thrust line that intersects the upper interface aligns with the line of action of thrust $F_B$. Then, it will always be the case, if point X is above the block, point Y is closer to the edge of the upper interface, and point Z is closer to where the line of action of the self-weight of the block ($W$) intersects the same interface.

The funicular thrust line in the case shown in Fig. 13c indicates the left edge of the interface to be a potential hinge point (note that point Z is at the edge of the interface). However, the equilibrium here is unrealistic as point Y is now outside the structure, and therefore the thrust $F_A$ cannot be transferred to the block. Fig. 13b shows the case where the thrust $F_A$ could have been transferred to the block while forming a potential hinge point. Note that point Y is at the edge of the interface.

What is observed here is that point X being above the block, on its own, cannot indicate the validity of the limit load indicated by the funicular thrust line (this will, in addition, require the construction of the free-body diagrams, as done above). In Fig. 13a and b, both the funicular thrust line and the free-body diagram indicate the existence of a safe load path although it could be argued that the funicular thrust line does not correctly represent the equilibrium (i.e, citing points Z and Y being apart). Whereas in Fig. 13c, the funicular thrust line identifies a potential hinge point but the equilibrium condition is unrealistic and therefore the limiting load indicated by the funicular thrust line is definitively incorrect; in fact, an overestimation. So are all the intermediate cases between Fig. 13b and c where the funicular thrust line would be well inside the structure (i.e., no potential hinge point identified by the funicular thrust line).

Recognizing that this exercise aims to identify erroneous funicular thrust lines, the conservative approach is to check all cases where point X is above the constituent block rather than (say) considering only the cases where the funicular thrust line indicates a potential hinge point. Thus we conjecture:

**Conjecture 2.** *Given only three forces are applied on a block in consideration, the point of intersection of the lines of action of the self-weight load and the thrusts at the interfaces (and/or external loads) being above the block indicate the possibility of the funicular thrust line overestimating the limit load of the structure.*

The above conjecture considers the position of points X, as this is readily observable from the funicular thrust line—these are the points where the weights are hung on the funicular. The positions of points Y are constructed

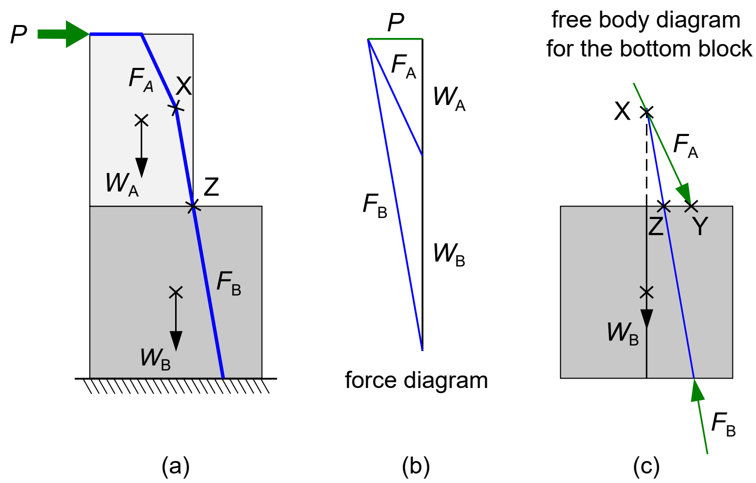


Figure 14: Over-estimation of the collapse load by the funicular thrust line: Point X corresponding to the bottom block is 'above' it, in (a). The free-body diagram of the bottom block, in (c), shows the thrust $F_A$ between the blocks acting at point Y, which is outside the interface between the two blocks. The force diagram corresponding to the funicular thrust line is in (b).

from the free-body diagram. Therefore, the application of this conjecture in practice would be by first checking the position of all the X points. If they are above the corresponding block, then extend the line of action of the thrust to get the point Y and observe where it intersects the corresponding interface.

Fig. 14 reproduces example in Fig. 8 as a specific example of applying Conjecture 2. Here, the point X of the block in consideration (bottom block) is above it and the funicular thrust line indicates a potential hinge point at the corresponding interface. This, therefore definitively leads to an overestimation of limit load by the funicular thrust line.

*5.3. Collapse load under-estimation*

Similarly, now consider the case from Fig. 10c where point X is below the constituent block but is within the structure. The free-body diagram and the funicular thrust line in Fig. 10c are reproduced in Fig. 15a, now with two more cases where the point of intersection of the funicular thrust line with the interface (point Z) and the point of action of the thrust $F_B$ (point Y), respectively, are at the edge of the lower interface. Without loss of generality,

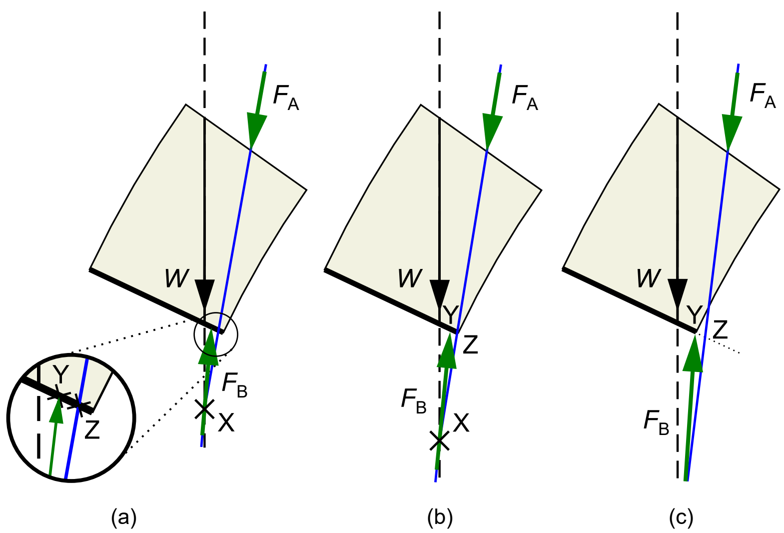


Figure 15: Possible cases for the position of the funicular thrust line when point X is below the block and point of action of the thrust $F_B$ within the lower interface. The lines of action of the equilibrating forces $F_A$, $F_B$, and $W$ on the block intersect at point X. The point of action of the thrust $F_B$ is point Y and the funicular thrust line intersects the interface at point Z. In (a) both points Y and Z are inside the structure; (b) point Z is at the boundary of the structure; (c) point Z is outside the structure while point Y is at the boundary of the structure.

the three cases are generated by increasing the vertical component of the thrust $F_A$ while the point of action of thrust $F_A$ at the top interface was kept the same.

In Fig. 15b, the funicular thrust indicates the right edge of the interface to be a potential hinge point (note that point Z is at the edge of the interface). However, the right edge would be a potential hinge point only in the case shown in Fig. 15c where point Y is at the edge of the interface. In the range of possible cases that fall between Fig. 15b and c, a valid load path exists although the funicular thrust line indicates no solution by virtue of the funicular thrust line lying outside the structure, and therefore underestimating the limit load.

What is observed here is that point X being below the block combined with the funicular thrust line passing through the edge of the corresponding interface (i.e., lower interface) indicates an underestimation of the limit load by the funicular thrust line. However, this cannot be used as definitive evidence of the limit load being underestimated as only a single block is considered here. A block elsewhere in the structure may be overestimating the load as the corresponding point X is above that block (see Appendix A). Thus we conjecture:

**Conjecture 3.** *Given only three forces are applied on the critical block in consideration, if (a) the point of intersection of the lines of action of the self-weight load and the thrusts at the interfaces (and/or external loads) is below the block, and (b) the funicular thrust line is passing through the edge of the lower interface of the block, then this indicates the possibility of the funicular thrust line underestimating the limit load.*

This conjecture can be used to identify funicular thrust lines where the limit load is underestimated. Fig. 16 presents an example where the conditions of Conjecture 3 are satisfied and isolating the corresponding block and drawing its free-body diagram indicates that a hinge is not formed at the interface between the blocks as suggested by the funicular thrust line.

## 6. Example: flat arch on two columns

A flat arch made of stone blocks and supported on two columns are now considered to demonstrate the superiority of thrust layouts over funicular thrust lines (see Fig. 17). The flat arch consists of five equally sized stone blocks and frictional sliding is ignored.

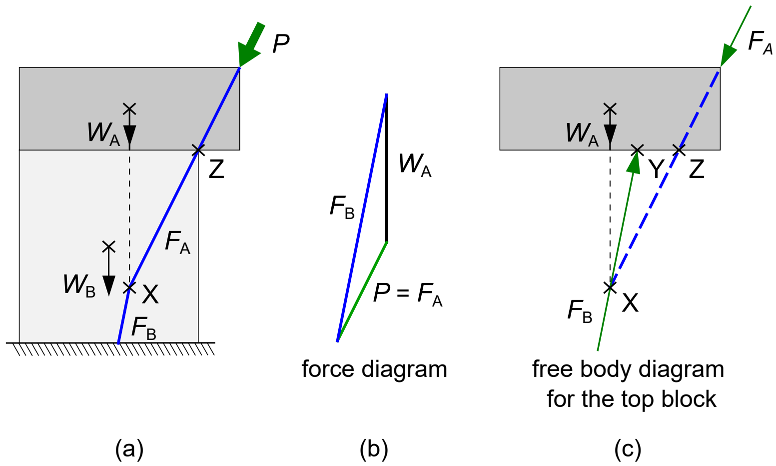


Figure 16: Under-estimation of the collapse load by the funicular thrust line: Point X corresponding to the top block is 'below' it, in (a). the free-body diagram of the top block, in (c), shows the thrust $F_B$ between the blocks acting at point Y, which is well within the interface between the two blocks. The force diagram corresponding to the funicular thrust line is in (b).

The funicular thrust line within the structure (see Fig. 17a) estimates the maximum central point load, $P$, of 9.91 kN. It is noted that the weight of the springer blocks is transferred to the columns at a point below them. Following Conjecture 3, this suggests that the load carrying capacity of the structure may be underestimated.

The thrust layout shown in Fig. 17b predicts the load carrying capacity is $P = 45.1$ kN. This value is determined to be the exact collapse load for the structure, via a rigid block analysis of the structure (Fig. 17c). Thrust layout is fully contained within the bounds of the structure and respects the block stereotomy. Note that the tensile forces within the springer blocks mobilize their weights within the corresponding block. In addition, the tensile forces within the keystone block allow the thrust layout to hug the extrados, creating the hinge points observed in the rigid block analysis. This significant increase in load-carrying capacity achieved by recognizing the tensile strength of the material is broadly consistent with what was observed by Boothby and Coronelli [23].

The funicular thrust lines and thrust layouts are constructed here using form-force duals (see force diagram in Fig. 18). Although the construction

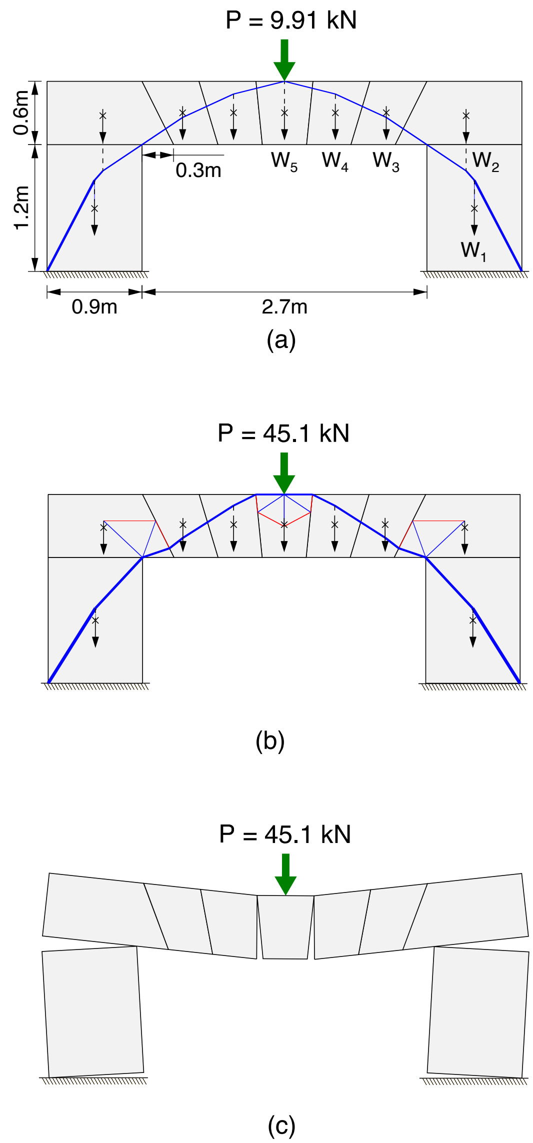


Figure 17: Flat arch on stone columns—solutions obtained using: (a) funicular thrust line; (b) thrust layout; and (c) rigid block method (all five blocks in the arch have a top breadth of 0.54 m and a bottom breadth of 0.42 m; a width of 1 m and material unit weight of 25 kN/m$^3$ are assumed).

of funicular thrust lines is fairly straightforward, thrust layout patterns may not be obvious at first glance. For example, the half-wheel pattern within the keystone is not foreseen by the conjectures presented. In recent work, Nanayakkara et al. [29] present an automated procedure for the generation of thrust layouts. Their work presents a collection of examples, further exploring the use of thrust layouts in the analysis of masonry gravity structures.

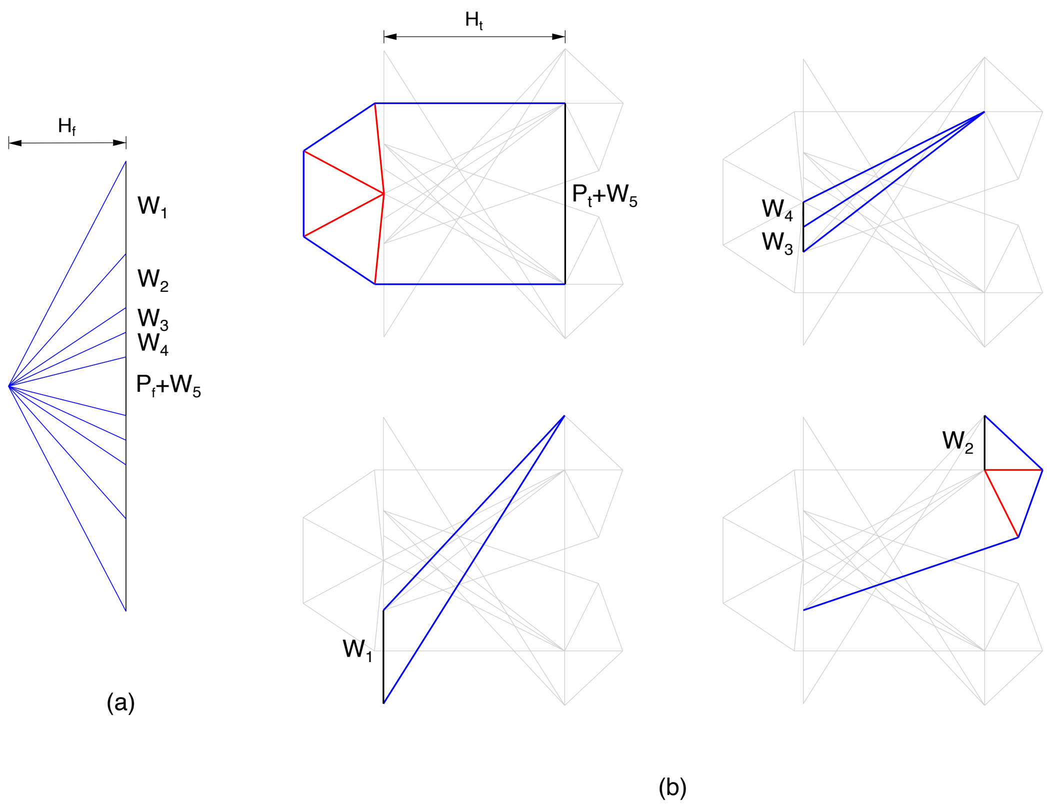


Figure 18: Dual force diagrams—solutions of the flat arch on stone columns example, obtained using (a) funicular thrust line; (b) thrust layout (deconstructed, in clockwise order from top-left, keystone block, left arch blocks, left springer block, and left column). $P_f$ an $P_t$ are collapse load estimates and $H_f$ an $H_t$ are horizontal thrusts at column base.

## 7. Discussion

Thrust layouts can be used for the analysis of masonry gravity structures where the block stereotomy is known; a structure is safe if a thrust layout fully contained within the structure can be found. One method of generating thrust layouts is by starting with a hanging chain model, and then using the two observations noted to identify locations where either an alternative load path is required or tension needs to be introduced; i.e., add struts and add/remove extra ties from the hanging chain model. However, this would be impractical where the geometry is complex and a large number of constituent blocks are involved. For such cases, user-friendly computer tools will be required to automatically generate thrust layouts, as has been the case for the generation of funicular thrust lines, e.g., [9, 30, 31].

Masonry gravity structures are generally statically indeterminate and thus have multiple possible 'safe' load paths. Knowing one of these would be satisfactory for an engineer to assess an existing structure (or to verify the design of a new one). In other words, although only one load path may exist in reality, knowing that particular load path is not necessary.

The thrust layout optimization (TLO) procedure presented recently by Nanayakkara et al. [29] automates the generation of thrust layouts. The presented numerical method solves an underlying linear programming (LP) problem, taking advantage of efficient and widely available LP solvers. Furthermore, the TLO procedure also takes account of the limited frictional capacity of block interfaces, albeit implicitly assuming associative friction. Thus the concerns of Bagi [22] are not addressed here, though this could be remedied by adopting an iterative solution scheme, e.g., the approach proposed in [32].

While noting that funicular thrust lines implicitly assume vertical tension-weak planes, Heyman suggests that a funicular thrust line would be valid for a monolithic continuum [13]. However, testing on monolithic arches made of rammed earth suggests that the failure planes of the arch are unlikely to be vertical [33, 34]. This suggests that a methodology that automatically identifies critical failure planes (e.g., [35, 36]) would be more appropriate for the analysis of form-resistant continua (e.g., arches formed using rammed earth construction). It is also noted that the effect of stereotomy on the minimum thickness of arches, without stereotomy considered a prior, has been extensively studied [37, 38, 39, 40, 12], and shows the effect of stereotomy to be limited in this particular case. Heyman's [41] classic solution considering infinitely many 'vertical-strips' gives a minimum arch thickness to radius ratio ($t/R$) of 0.106, for semi-circular arches. Similarly, considering radial joints, Ochsendorf [12] calculates a minimum $t/R$ of 0.1075. Having the voussoir joints variable, Gaspar [39] calculates a minimum $t/R$ of 0.0819. But, when the friction capacity is considered the stereotomy effect is found to be limited: For a friction coefficient of unity, variable voussoir joints give a minimum $t/R$ of 0.1044 [40].

Thrust networks are the equivalent three-dimensional extension of funicular thrust lines, and similar shortcomings exist there too. Fantin and Ciblac [42] extend thrust networks with additional ‘partial branches’ to account for solutions where the forces on a block do not converge to a point, whereas thrust networks restrict the domain of acceptable solutions to where all forces on a block coincide at a point. This, however, does not appear in the two-dimensional problem as the blocks are in equilibrium under only three forces and therefore must meet at a point to satisfy equilibrium. Furthermore, Barsi et al. [20] map the funicular thrust lines to the classic membrane solution (in 3D) and the line of resistance to thrust surfaces (in 3D).

## 8. Conclusions

Heyman’s ‘safe theorem’ is widely used in the assessment of masonry gravity structures. In developing his theorem, Heyman used a funicular thrust line to represent the equilibrium of a masonry gravity structure. However, as noted in this contribution, there are limitations associated with using a funicular thrust line to represent the state of equilibrium of a masonry gravity structure. These limitations arise from not taking account of block stereotomy, which can lead to either under- or over-estimation of the collapse load of a masonry gravity structure, contrary to the commonly held belief that the thrust line method will generally give safe solutions. Furthermore, the implicit reliance on tensile strength when working with funicular thrust lines is not clear to users.

Here, the notion of a ‘thrust layout’ is proposed. Block stereotomy is explicitly taken into account in a thrust layout, with tensile forces allowed within constituent blocks, but not across the weak interfaces between blocks. Thrust layouts can be used in the application of Heyman’s safe theorem to any structure, as this now appropriately represents the equilibrium of the structure. Furthermore, similar to funicular thrust lines, thrust layouts visualize a flow of forces within a structure. Thus, in contrast to the ‘line of resistance’ presented by Moseley, a thrust layout enables the structural engineer to clearly grasp how a masonry gravity structure safely carries applied loads.

## Acknowledgements

MG acknowledges the financial support provided by the Engineering and Physical Research Council under grant reference EP/T001305/1.



## References

[1] J. Heyman, The stone skeleton, Int J Solids Struct 2 (2) (1966) 249–279. doi:10.1016/0020-7683(66)90018-7.

[2] P. Block, M. DeJong, J. Ochsendorf, As hangs the flexible line: Equilibrium of masonry arches, Nexus Netw J 8 (2) (2006) 13–24. doi:10.1007/s00004-006-0015-9.

[3] K.-E. Kurrer, The History of the Theory of Structures: Searching for Equilibrium, 2nd Edition, Wiley, 2018.

[4] R. Graefe, The catenary and the line of thrust as a means for shaping arches and vaults, in: B. Addis (Ed.), Physical Models: their historical and current use in civil and building engineering design, Ernst & Sohn, 2021, Ch. 3, pp. 79–126.

[5] J. A. Ochsendorf, P. Block, Designing unreinforced masonry, in: E. Allen, W. Zalewski (Eds.), Form and Forces: Designing Efficient, Expressive Structures, Wiley, 2009, Ch. 8, pp. 215–245.

[6] J. Chilton, C.-C. Chuang, Rooted in nature: Aesthetics, geometry and structure in the shells of Heinz Isler, Nexus Netw J 19 (3) (2017) 763–785. doi:10.1007/s00004-017-0357-5.

[7] P. Block, J. Ochsendorf, Thrust network analysis: A new methodology for three-dimensional equilibrium, J Int Assoc Shell Spat Struct 48 (3) (2007) 8.

[8] V. Paris, G. Ruscica, G. Mirabella Roberti, Graphical modelling of hoop force distribution for equilibrium analysis of masonry domes, Nexus Netw J 23 (4) (2021) 855–878. doi:10.1007/s00004-021-00556-x.

[9] A. Kilian, J. Ochsendorf, Particle-spring systems for structural form finding, J Int Assoc Shell Spat Struct 46 (147) (2005) 8.

[10] S. Bagrianski, A. B. Halpern, Form-finding of compressive structures using Prescriptive Dynamic Relaxation, Comput Struct 132 (2014) 65–74. doi:10.1016/j.compstruc.2013.10.018.

[11] J. Heyman, The Masonry Arch, Ellis Horwood, Chichester, UK, 1982.

[12] J. Ochsendorf, Collapse of masonry structures, Ph.D. thesis, University of Cambridge, Cambridge, UK (2002).

[13] J. Heyman, La coupe des pierres, in: K.-E. Kurrer, W. Lorenz, V. Wetzk (Eds.), Proc. 3rd Int. Congr. Constr. Hist., Cottbus, Germany, 2009, pp. 807–812.

[14] J. Heyman, Equilibrium of masonry arches, Proc Inst Civ Eng Eng Comput Mech 163 (3) (2010) 129–133. doi:10.1680/eacm.2010.163.3.129.

[15] J. Heyman, Leaning towers, Meccanica 27 (1992) 153–159. doi:10.1007/BF00430041.

[16] H. Alexakis, N. Makris, Limit equilibrium analysis of masonry arches, Arch Appl Mech 85 (2015) 1363–1381. doi:10.1007/s00419-014-0963-6.

[17] J. Ochsendorf, The masonry arch on spreading supports, Struct Eng 84 (2) (2006) 29–35.

[18] N. Grillanda, A. Chiozzi, G. Milani, A. Tralli, NURBS solid modeling for the three-dimensional limit analysis of curved rigid block structures, Comput Methods Appl Mech Eng 399 (2022) 115304. doi:10.1016/j.cma.2022.115304.

[19] F. Marmo, Archlab: a matlab tool for the thrust line analysis of masonry arches, Curved Layer Struct 8 (1) (2021) 26–35. doi:10.1515/cls-2021-0003.

[20] F. Barsi, R. Barsotti, S. Bennati, T. Ciblac, Investigating the relation between thrust networks and thrust surfaces for masonry domes subjected to vertical loads: A case study, Int J of Archit Heritage 0 (0) (2022) 1–19. doi:10.1080/15583058.2022.2101159.

[21] M.-K. Nikolinakou, A. J. Tallon, J. A. Ochsendorf, Structure and form of early gothic flying buttresses, Eur J Environ Civ Eng 9 (9-10) (2010) 1191–1217. doi:10.1080/17747120.2005.9692807.

[22] K. Bagi, When Heyman's Safe Theorem of rigid block systems fails: Non-Heymanian collapse modes of masonry structures, Int J Solids Struct 51 (14) (2014) 2696–2705. doi:10.1016/j.ijsolstr.2014.03.041.

[23] T. E. Boothby, D. Coroneli, The stone skeleton: a reappraisal, Heritage 7 (2024) 2265–2276. doi:10.3390/heritage7050107.

[24] T. E. Boothby, Analysis of masonry arches and vaults, Prog Struct Eng Mat 3 (3) (2001) 246–256. doi:10.1002/pse.84.

[25] H. Moseley, The Mechanical Principles of Engineering and Architecture, Longman, Brown, Green, and Longmans, New York, 1843.

[26] M. Milankovitch, Theorie der druckkurven, Zeitschrift für Mathematik und Physik 55 (1907) 1–27.

[27] F. Foce, Milankovitch's Theorie der druckkurven: Good mechanics for masonry architecture, Nexus Netw J 9 (2) (2007) 185–210. doi:10.1007/s00004-007-0039-9.

[28] P. Fuentes, Mechanics of flying buttresses: the case of the cathedral of mallorca, J Mech Mater Struct 13 (5) (2018) 617–630. doi:10.2140/jomms.2018.13.617.

[29] K. I. U. Nanayakkara, A. Liew, M. Gilbert, Application of thrust layout optimization to masonry structures, Proc Math Phys Eng Sci 479 (2273) (2023) 20230053. doi:10.1098/rspa.2023.0053.

[30] P. Block, T. Ciblac, J. Ochsendorf, Real-time limit analysis of vaulted masonry buildings, Comput Struct 84 (29) (2006) 1841–1852. doi:10.1016/j.compstruc.2006.08.002.

[31] H. E. Fairclough, L. He, T. J. Pritchard, M. Gilbert, LayOpt: An educational web-app for truss layout optimization, Struct Multidiscip Optim 64 (4) (2021) 2805–2823. doi:10.1007/s00158-021-03009-8.

[32] M. Gilbert, C. Casapulla, H. M. Ahmed, Limit analysis of masonry block structures with non-associative frictional joints using linear programming, Comput. Struct. 84 (13-14) (2006) 873–887. doi:10.1016/j.compstruc.2006.02.005.

[33] T. Michiels, R. Napolitano, S. Adriaenssens, B. Glisic, Comparison of thrust line analysis, limit state analysis and distinct element modeling to predict the collapse load and collapse mechanism of a rammed earth arch, Eng Struct 148 (2017) 145–156. doi:10.1016/j.engstruct.2017.06.053.

[34] F. Loccarini, G. Ranocchiai, T. Rotunno, M. Fagone, Experimental and numerical analyses of strengthened rammed earth masonry arches, Comput Struct 239 (2020) 106329. doi:10.1016/j.compstruc.2020.106329.

[35] J. Valentino, M. Gilbert, M. Gueguin, C. C. Smith, Limit analysis of masonry walls using discontinuity layout optimization and homogenization, Int J Numer Meth Eng 124 (2) (2023) 358–381. doi:10.1002/nme.7124.

[36] N. A. Nodargi, P. Bisegna, A unifying computational approach for the lower-bound limit analysis of systems of masonry arches and buttresses, Eng Struct 221 (2020) 110999. doi:10.1016/j.engstruct.2020.110999.

[37] D. Aita, A. Sinopoli, Two different approaches for collapse of non-symmetric masonry arches: Monasterio's treatment versus limit equilibrium analysis, J Eng Mech-ASCE 147 (10) (2021) 04021071. doi:10.1061/(ASCE)EM.1943-7889.0001989.

[38] D. Aita, R. Barsotti, S. Bennati, Looking at the collapse modes of circular and pointed masonry arches through the lens of Durand-Claye's stability area method, Arch Appl Mech 89 (8) (2019) 1537–1554. doi:10.1007/s00419-019-01526-z.

[39] O. Gáspár, A. A. Sipos, I. Sajtos, Effect of stereotomy on the lower bound value of minimum thickness of semi-circular masonry arches, Int J of Archit Heritage 12 (6) (2018) 899–921. doi:10.1080/15583058.2017.1422572.

[40] O. Gáspár, I. Sajtos, A. A. Sipos, Friction as a geometric constraint on stereotomy in the minimum thickness analysis of circular

and elliptical masonry arches, Int J Solids Struct 225 (2021) 111056. doi:10.1016/j.ijsolstr.2021.111056.

[41] J. Heyman, The safety of masonry arches, Int J Mech Sci 11 (4) (1969) 363–385. doi:10.1016/0020-7403(69)90070-8.

[42] M. Fantin, T. Ciblac, Extension of thrust network analysis with joints consideration and new equilibrium states, Int J Space Struct 31 (2-4) (2016) 190–202. doi:10.1177/0266351116661814.

## Appendix A. Example: Stack-of-four blocks

The funicular thrust line drawn for the stack-of-four-blocks example (see Fig. A.19) indicates a situation where the self-weights $W_B$ and $W_C$ are mobilized outside their corresponding blocks, but still within the structure. In the case of block B, the lines of action of the three equilibrating forces on the block intersect at a point above the block indicating the possibility of an overestimation of the load capacity. The corresponding intersection point in block C is below the block, indicating the possibility of an underestimation of the load capacity. The overall impact of these two scenarios cannot be readily predicted by simply looking at the funicular thrust line.

Since the funicular thrust line does not correctly represent the equilibrium of the structure and the problematic interfaces (between blocks A and B and C and D) have been identified, this can be further investigated.

Considering the moment equilibrium of block A about point Z, the force $P$ should be less than 4.5 units to prevent overturning about point Z. Similarly, to prevent rocking about point Y, the force $P$ should be greater than 6.16 units (considering the moment about point Y considering blocks A, B, and C). Therefore, there is no valid solution for this assembly of blocks although a valid funicular thrust line is constructed. Therefore, the overall effect is a load overestimation.

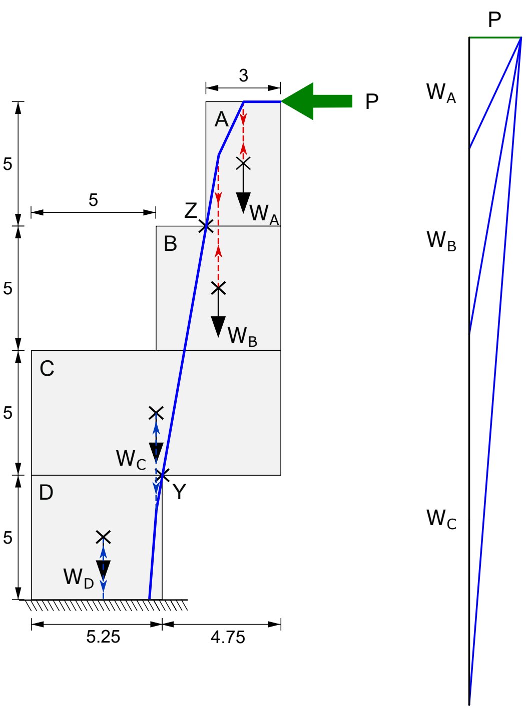


Figure A.19: A funicular thrust line indicating simultaneous over and under-estimation of load carrying capacity. A stack of four blocks with geometry as indicated is considered. The Corresponding force diagram is also shown. (Compression and tension forces are shown in blue and red respectively. For $W_A$, $W_B$, $W_C$ and $W_D$ of 15, 25, 50, and 26.25 units, $P_1$ is 7 units.)